Title
STUDY OF INTERMEDIATE STATES PRODUCED BY RADIATIVE DECAYS OF Y

Author
Trilling, George H.

Publication Date
1976-10-01

Talk presented at the Summer Institute
on Particle Physics, SLAC, Stanford,
CA, August 2 - 13, 1976

LBL-5535
c.1

STUDY OF INTERMEDIATE STATES PRODUCED BY RADIATIVE DECAYS OF ψ

George H. Trilling

October 1976

Prepared for the U. S. Energy Research and
Development Administration under Contract W-7405-ENG-48

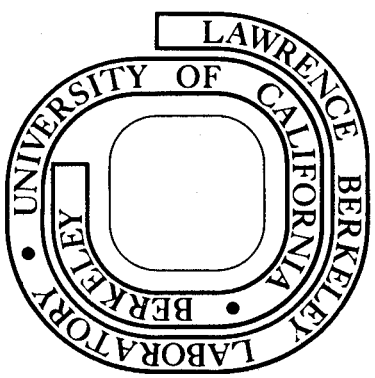

LBL-5535
c.1

DISCLAIMER

LBL-5535

STUDY OF INTERMEDIATE STATES PRODUCED BY RADIATIVE DECAYS OF ψ'

George H. Trilling

Department of Physics and Lawrence Berkeley Laboratory
University of California, Berkeley, California 94720

I. INTRODUCTION

I shall, in this report, discuss recent experimental information on narrow states, intermediate in mass between the ψ and the ψ', which are produced by radiative decays of the ψ'. The data on which this information is based consists of about 350,000 ψ' decays detected by the SLAC/LBL magnetic detector operating at SPEAR. This detector has been described elsewhere,[1] and I shall not go into its details here.

In the present conventional interpretation of the ψ and ψ' particles as bound states of a charmed quark and charmed antiquark ($c\bar{c}$), the predicted properties of those $c\bar{c}$ states which might be expected to be lower in mass than the ψ' are given in Table I. The ψ and ψ' correspond to the $J^{PC} = 1^{--}$ state (with the ψ' presumably a radial excitation). Those states with charge parity $C = +1$ are all possible decay products (X) in the process

$$\psi' \rightarrow \gamma X \quad . \tag{1}$$

If we restrict the symbol X to those states intermediate in mass between the ψ' and the ψ, we might expect these to consist of the 2^1S_0 and the 1^3P_0, 1^3P_1, 1^3P_2 states. (We assume here that the 1^1S_0 state lies below the ψ.) Thus one may expect to find four X states with the properties $J^{PC} = 0^{-+}$, 0^{++}, 1^{++}, 2^{++}. Presumably the same dynamical effects which lead to the narrow ψ and ψ' widths also apply to the X's; hence their observed widths are expected to be determined purely by the resolution of the detector.

The methods which have been used in the magnetic detector at SPEAR to study X states are the following:

(1) Study of inclusive photon spectra with good resolution to search for monoenergetic photon lines.

(2) Study of the cascade processes,

$$\begin{array}{l} \psi' \rightarrow \gamma_1 X \\ \qquad\quad \big|\rightarrow \gamma_2 \psi \\ \qquad\qquad\quad \big|\rightarrow e^+e^- \text{ or } \mu^+\mu^- \ . \end{array} \qquad (2)$$

(3) Study of hadronic decays of X states,

$$\begin{array}{l} \psi' \rightarrow \gamma X \\ \qquad\quad \big|\rightarrow \text{hadrons} \ . \end{array} \qquad (3)$$

In the subsequent sections, the results of these approaches are discussed in some detail.

II. INCLUSIVE PHOTON SPECTRA

The detection of monoenergetic photons emitted in ψ' decays is a conceptually simple and natural method to search for narrow intermediate states. The anticipated results of such a study would be the identification of various X states, and the determination of ψ' branching ratios for decay into each X state detected. The principal experimental difficulty arises from the enormous background of photons from π^0 decay, especially at the low energies where one expects to find the desired monoenergetic photons.

For such a study, the magnetic detector was used as a pair spectrometer,[2] the beam pipe wall and scintillation counter surrounding that wall serving as the thin converters, and the cylindrical spark chambers being used to measure the momenta of the outgoing electron and positron. The efficiency for detecting photons in this manner rises rapidly from zero below 120 MeV to $\sim 1\%$ at 200 MeV and thence slowly to about 2% at the highest photon energies. The resolution σ is about 4 MeV at 200 MeV. The results for both ψ and ψ' photon spectra are shown in Fig. 1. The general shapes of both spectra are the same (as might be expected from the fact that most ψ' decays lead to a ψ), but the ψ' spectrum exhibits

a clear spike at $E_\gamma = 261 \pm 10$ MeV (corresponding to $M_\chi = 3413 \pm 11$ MeV) with a width consistent with the resolution.[3] The sharp drop-off below 250 MeV is due to the loss of efficiency; and indeed this experiment is incapable, from the inclusive spectrum, to make any useful statement about monoenergetic photons of significantly lower energy. The ψ' branching ratio corresponding to this signal[4] is 0.075 ± 0.026, where the quoted error arises principally from systematic uncertainties in the background subtraction and in the evaluation of the relevant efficiencies.

It may be noted that the experiment of Badtke et al.,[5] in the other experimental area of SPEAR, using NaI crystals to detect photons, has a much lower energy threshold. Thus this group has reported monoenergetic lines at $E_\gamma = 256$, 168 and 121 MeV, all with an uncertainty of ± 7 MeV (corresponding to $M_\chi = 3418$, 3512 and 3561 MeV). The corresponding branching ratios are 0.1 ± 0.04, 0.09 ± 0.03, 0.08 ± 0.03 respectively.[4] The first of these is, within the substantial uncertainties of both measurements, compatible with the above magnetic-detector value. As will be seen below, the other two states have also been observed by the other methods in which the magnetic detector has been used to study X states.

III. CASCADE DECAY OF ψ'

The processes (2) were precisely those from which the first evidence for intermediate states was obtained by the DESY-DASP group.[6] In addition to providing a very clean way to identify those X states which have significant branching ratios for the decays $X \to \gamma\psi$, these processes can potentially yield the most powerful data for determinations of the spins of these same X states.[7] The main difficulty of such a study is the removal of background from the processes

$$\psi' \to \pi^o\pi^o\psi \to \gamma\gamma\gamma\gamma\psi \ ,$$

$$\psi' \to \eta\psi \to \gamma\gamma\psi \ .$$

The recent results[2] from the SLAC/LBL magnetic detector are obtained from

a study of events in which either γ_1 or γ_2 in (2) are converted into an e^+e^- pair in the manner already described in Section II, and the momentum of the unconverted photon is then determined by momentum-energy balance. To sharpen the resolution, a kinematic fit is made in which the dilepton pair is constrained to the ψ mass. Details concerning the removal of the above-mentioned backgrounds are given in Ref. 2; in the subsequent discussion we assume that such backgrounds have been removed. The remaining sample consists of 21 events.

For each event in the sample, there are two possible X masses depending upon which photon is assumed to arise from the ψ' decay and which from the X decay. The correct choice can in principle be made with adequate data from the requirement of small X widths. The scatter plot of the low $\psi\gamma$ mass versus the high $\psi\gamma$ mass for the 21-event sample is shown in Fig. 2, with the projections on both axes also exhibited. There are clear peaks at 3504 ± 10 MeV and 3543 ± 10 MeV with branching ratio products $B(\psi' \rightarrow \gamma X)B(X \rightarrow \gamma\psi)$ of 0.024 ± 0.008 and 0.01 ± 0.006 respectively, accounting for 16 of the 21 events. For both of these states, the required small width provides a unique resolution of the $\psi\gamma$ mass ambiguity in favor of the high mass solution. This choice also agrees well with the data of Badtke et al.[5] and with the results from studies of X hadronic modes discussed in Section IV. Of the remaining events, one lies at 3413 MeV (high $\psi\gamma$-mass solution) which, as discussed earlier, corresponds to a known X state (although a single event could just be background) and corresponds to a branching ratio product of 0.002 ± 0.002. Finally the remaining four events are all consistent with a single mass of 3455 ± 10 MeV (high $\psi\gamma$ solution) and a branching ratio product of 0.008 ± 0.004. It is also possible to throw out one of these four events as background and retain the other three at a common mass value of 3340 ± 10 MeV (low $\psi\gamma$-mass solution). Although this 3455 MeV (or 3340 MeV) signal looks reasonably solid in Fig. 2, it differs from the other signals in one important respect: as will be discussed later, there is no indication

for any observable hadronic mode at either of these masses, nor is there any clear evidence for this mode in the inclusive photon spectra in which the other X states show up. Thus this state clearly requires confirmation before it can be considered as established.

IV. HADRONIC DECAYS OF X

A. General Features

Hadronic decays of X states can be identified for those decay modes consisting only of charged outgoing particles all of which are detected in the apparatus. The specific decay modes studied are the following:

$$X \to \pi^+\pi^-\pi^+\pi^- \qquad (4a)$$

$$\to \pi^+\pi^- K^+K^- \qquad (4b)$$

$$\to \pi^+\pi^-\pi^+\pi^-\pi^+\pi^- \qquad (4c)$$

$$\to \pi^+\pi^- \qquad (4d)$$

$$\to K^+K^- \qquad (4e)$$

$$\to \pi^+\pi^- p\bar{p}\,. \qquad (4f)$$

Identification of reaction (3) is achieved, without detecting the photon, through energy and momentum balance. The major problem in the application of this procedure is the separation of $\psi' \to \gamma X$ from $\psi' \to \pi^o X$ where X is a final state consisting of one of the groups of hadrons listed in (4). Fortunately this separation is reasonably straightforward for three reasons: (a) Decay modes of the form $\psi' \to \pi^o$ + all charged particles have relatively small branching ratios; (b) such decay modes have a π^o spectrum spread over a wide range of energies whereas the photons in (3) are monoenergetic with relatively small energy; (c) the measurement of missing-mass-squared by which one distinguishes a missing photon from a missing pion is most precise when the energy taken up by the missing or neutral system is small -- this is just the case in reaction (3). These points have already been discussed in the paper of Feldman et al.,[3] and the recent work based on the much larger statistics now available confirms the validity of the γ-π^o separation.

We do not here go into great detail on the fine points of the analysis, but do mention the following relevant elements:

(i) The X masses are determined from a one-constraint kinematic fit to reactions (3) and (4) using the bubble-chamber program SQUAW.

(ii) Care is used to remove certain prominent backgrounds:

(a) $\psi' \to \gamma X \to \gamma\pi^+\pi^-\pi^+\pi^-$, $\gamma\pi^+\pi^-K^+K^-$

Background: $\psi' \to \pi^+\pi^-\psi \to \pi^+\pi^-\mu^+\mu^-$, $\pi^+\pi^-e^+e^-$

(b) $\psi' \to \gamma X \to \gamma\pi^+\pi^-\pi^+\pi^-\pi^+\pi^-$

Background: $\psi' \to \pi^+\pi^-\psi \to \pi^+\pi^-\pi^+\pi^-\pi^+\pi^-$, $\pi^+\pi^-\pi^+\pi^-\pi^+\pi^-\pi^o$

(c) $\psi' \to \gamma X \to \gamma\pi^+\pi^-$, γK^+K^-

Background: $\psi' \to e^+e^-$, $\mu^+\mu^-$, γe^+e^-, $\gamma\mu^+\mu^-$

(iii) Time-of-flight information plus the kinematic fit are used to identify the X decay modes $\pi^+\pi^-K^+K^-$ and $\pi^+\pi^-p\bar{p}$. The kinematic fit alone is usually adequate to separate $X \to \pi^+\pi^-$ from $X \to K^+K^-$.

(iv) In the calculation of branching ratios corrections have been made for the effects of the various cuts used.

The mass spectra corresponding to the various final states (4) are shown in Figs. 3 and 4. On the basis of these spectra one can make the following remarks:

(1) All the mass spectra show a prominent peak at $M_X = 3415 \pm 10$ MeV.

(2) The 4π and $\pi\pi KK$ spectra also show clear peaks at $M_X = 3500 \pm 10$ MeV and 3550 ± 10 MeV. These three mass values are in good agreement with those observed by the other techniques previously discussed.

(3) The 6π spectrum above the 3415 MeV peak is compatible with populations from the above two states, although they are not clearly resolved.

(4) The combined $\pi^+\pi^-$ and K^+K^- spectra show a fairly clear peak at 3550 MeV but no significant signal at 3500 MeV.

(5) There is no evidence for any signal at 3450 MeV, the state suggested by the cascade decay data of Fig. 2.

(6) The peaks at the upper end of the 4π, $\pi\pi K\bar{K}$ and $\pi\pi p\bar{p}$ spectra do not

come from X states, but rather correspond to the direct decay modes $\psi' \to 4\pi$, $\pi\pi K\bar{K}$, $\pi\pi p\bar{p}$. There is also a small but finite contribution from $\psi' \to 6\pi$ at the upper end of the 6π spectrum. The absence of such population at the upper end of the $\pi^+\pi^-$, K^+K^- spectrum is not in itself proof of the absence of the direct modes $\psi' \to \pi^+\pi^-$, K^+K^-, because cuts used to remove $\psi' \to e^+e^-$, $\mu^+\mu^-$ background also remove $\psi' \to \pi^+\pi^-$, K^+K^-.

B. Study of the X(3415) Decays

Table II shows preliminary values of branching ratios for the various identified decay modes. To obtain the X branching ratios, I have divided the branching ratio products by the total $\psi' \to \gamma X(3415)$ branching ratio of 0.075 ± 0.026 discussed in Section II.

Figure 5 shows the $\pi^+\pi^-$ and $K^\pm\pi^\mp$ spectra from the $\pi^+\pi^-\pi^+\pi^-$ and $\pi^+\pi^-K^+K^-$ decay modes, from which it is clear that the ρ and $K^*(891)$ are the only prominent resonances. Remarkably (since there are no obvious selection rules which forbid these processes), there is no significant $\rho\rho$ or $K^*(891)\bar{K}^*(891)$ signal: the ρ and K^* almost always seem accompanied by nonresonant meson pairs.

Other interesting properties can be summarized as follows:

(1) The G parity is even and charge parity is even; hence the isospin must be even. The K^+K^- decay mode thus requires that $I = 0$.

(2) The observed equality of $\pi^+\pi^-$ and K^+K^- branching ratios agrees with expectations for an SU(3) singlet assignment for the X(3415).

(3) The observed ratio of $\dfrac{X \to \rho\pi^+\pi^- \to \pi^+\pi^-\pi^+\pi^-}{X \to K^*(891)K\pi \to K^+\pi^-K^-\pi^+}$ decay rates, namely 1.12 ± 0.55, is also in agreement with the SU(3) singlet prediction of 9/8.

(4) The branching ratios for X(3415) to $\pi^+\pi^-$, $\pi^+\pi^-\pi^+\pi^-$ and $\pi^+\pi^-\pi^+\pi^-\pi^+\pi^-$ are very similar to the corresponding values observed for ψ decay to $\pi^+\pi^-\pi^o$, $\pi^+\pi^-\pi^+\pi^-\pi^o$, $\pi^+\pi^-\pi^+\pi^-\pi^+\pi^-\pi^o$ respectively.[8] (In making this comparison a π^o is added to go from X to corresponding ψ decay modes to take account of the opposite G parities.)

C. The X(3500) and X(3550) Decays

Tables III and IV show branching ratio products for X(3500) and X(3550). Estimates of the X branching ratios, obtained by using the ψ' branching ratio results of Badtke et al.[5] are also given in Tables III and IV. The prominence of the radiative mode $\gamma\psi$ is evident for both X states. The importance of this mode relative to the normal hadronic modes is very reminiscent of the prominence of the decay modes $\psi' \to \psi$ + anything relative to the standard ψ' hadronic modes. Although ρ and $K^*(891)$ production are significant pieces of the $\pi^+\pi^-\pi^+\pi^-$ and $\pi^+\pi^-K^+K^-$ modes for both X(3500) and X(3550) it is again true that both $\rho\rho$ and $K^*\bar{K}^*$ seem absent. The ratios of $\rho\pi\pi$ to $K^*K\pi$ again satisfy, to within the rather large statistical uncertainties, the SU(3) singlet predictions.

V. SPIN INFORMATION

For the hadronic modes, one can measure the distribution of θ, the angle between the beam direction and the outgoing photon. The general form is,[7]

$$W(\theta)d\cos\theta = 1 + A\cos^2\theta \qquad (5)$$

where $|A| \leq 1$.

The value of A can be unambiguously predicted only for spin $J = 0$, namely $A = 1$. For spins 1 and 2, there can be several multipoles in the amplitude and the predictions are ambiguous. However if one assumes that only the electric dipole contributes significantly, one obtains,

$$A = -1/3 \qquad J = 1$$

$$A = 1/13 \qquad J = 2$$

The actual experimental results, based on using all the observed hadronic decay modes are as follows[8]:

$$X(3415) \qquad A = 1.4 \pm 0.4$$

$$X(3500) \qquad A = 0.1 \pm 0.4$$

$$X(3550) \qquad A = 0.3 \pm 0.4$$

Figure 6b and Fig. 7 show the distributions of $|\cos\theta|$ from which

the above values of A are derived. Figure 6a, which applies only to the $\chi(3415) \to \pi^+\pi^-$ or K^+K^- mode shows the distribution of $|\cos\theta'|$ where θ' is the angle between dimeson line and the photon. This distribution is expected to be isotropic for $J = 0$, and would normally contain terms in $\cos^2\theta'$ and $\cos^4\theta'$ if $J = 2$ (the next lowest allowed spin for state with a $\pi^+\pi^-$ or K^+K^- decay mode). Unfortunately the statistics are small, but there is no obvious deviation from isotropy.

The main conclusion from these results is that only the $\chi(3415)$ gives a good fit to spin zero. For the $\chi(3500)$, the radiative cascade decay process with its additional useful variables can potentially provide much more conclusive information on the spin.[7] Preliminary analysis of events in which the photons are detected in the shower counters of the magnetic detector (a much larger sample than that discussed in Section III, where one photon is required to convert into an e^+e^- pair prior to reaching the first spark chamber) appears to rule out spin zero and thus confirms the tentative conclusion based on the γ angular distribution in the hadron decays.

Guided by the predictions of the charm model (see Table I), the fact that $\pi^+\pi^-$, K^+K^- decay modes imply $J^P = 0^+, 2^+, \ldots$, and the previous discussions of angular distributions, one is led to a favored assignment:

$$\chi(3415) \qquad J^{PC} = 0^{++}$$
$$\chi(3500) \qquad J^{PC} = 1^{++}$$
$$\chi(3550) \qquad J^{PC} = 2^{++} \ .$$

Complete experimental confirmation of these assignments is obviously desirable, but will not come easily with the present detectors.

VI. CONCLUDING REMARKS

From the totality of the information given we can come to the following conclusions:

1. There are three clearly-established states between the ψ' and the ψ at masses of 3415, 3500 and 3550 MeV (an actual average of all data done

by G. Feldman[10] gives values of 3414, 3508 and 3552 MeV for the masses). Thus the ambiguity between 3270 and 3500 MeV as the mass of the first state seen in the cascade decay mode[6] is removed.

2. The three above states all show significant hadronic decay modes. The radiative mode $X \to \gamma\psi$ seems the dominant one for the X(3500), very substantial for the X(3550), and, at most, of the same order as individual hadronic modes for the X(3415).

3. The limited information on isospin and SU(3) supports for the X states the $I = 0$ and SU(3) singlet properties predicted by the $c\bar{c}$ model.

4. The cascade process suggests the existence of another X state at a mass of 3455 or perhaps 3550 MeV. There is no evidence for hadronic decay modes of such a state.

5. There is a preferred but not conclusively established set of spin assignments, namely $J^P = 0^+$, 1^+ and 2^+ for the X(3415), X(3500) and X(3550) respectively. Thus of the states expected from the $c\bar{c}$ model the pseudoscalar is missing. Perhaps the 3455 MeV state seen in the cascade process is in fact this pseudoscalar, but there are no experimental data to support this hypothesis.

6. In my view, further substantial progress in this area can only come from coupling a much superior neutrals detector to a charged-particle detector at least as good as the present SLAC/LBL instrument.

The results presented in this paper come from the work of the SLAC/LBL collaboration, whose membership is: G. S. Abrams, M. S. Alam, A. M. Boyarski, M. Breidenbach, W. C. Carithers, W. Chinowsky, S. C. Cooper, R. G. DeVoe, J. M. Dorfan, G. J. Feldman, C. E. Friedberg, D. Fryberger, G. Goldhaber, G. Hanson, J. Jaros, A. D. Johnson, J. A. Kadyk, R. R. Larsen, D. Lüke, V. Lüth, H. L. Lynch, R. J. Madaras, C. C. Morehouse, H. K. Nguyen, J. M. Paterson, M. L. Perl, I. Peruzzi, M. Piccolo, F. M. Pierre, T. P. Pun, P. Rapidis, B. Richter, B. Sadoulet, R. H. Schindler, R. F. Schwitters, J. Siegrist, W. Tanenbaum, F. Vannucci, J. S. Whitaker, and J. E. Wiss. I am

particularly indebted to J. S. Whitaker, W. Tanenbaum, B. Sadoulet and A. D. Johnson for valuable discussions.

FOOTNOTES AND REFERENCES

1. J.-E. Augustin et al., Phys. Rev. Lett. 34, 764 (1975).
2. J. S. Whitaker et al., LBL-5382, submitted to Phys. Rev. Lett.
3. Evidence for this state was first reported by G. J. Feldman et al., Phys. Rev. Lett. 35, 821 (1975).
4. For efficiency determinations, the angular distribution relative to the beam has been assumed to be $(1 + \cos^2 \theta)$ for the 260 MeV photon and isotropic for the others, in accordance with the results discussed in Section V.
5. D. H. Badtke et al., paper submitted to the XVIIIth International Conference on High Energy Physics, Tbilisi, USSR (1976).
6. W. Braunschweig et al., Phys. Letters 57B, 407 (1975); also W. Tanenbaum et al., Phys. Rev. Lett. 35, 1323 (1975).
7. G. Karl, S. Meshkov and J. L. Rosner, Phys. Rev. D13, 1203 (1976); L. S. Brown and R. N. Cahn, Phys. Rev. D13, 1195 (1976).
8. B. Jean-Marie et al., Phys. Rev. Lett. 36, 291 (1976).
9. The coefficients of $\cos^2 \theta$ here differ slightly from values quoted earlier because we have used a slightly different and larger event sample to reduce as much as possible the statistical errors.
10. G. Feldman, Lectures at the SLAC Summer Institute (1976).

This work was done with support from the U.S. Energy Research and Development Administration.

Table I. Expected $c\bar{c}$ states.

State	J^{PC}	Reaction (1) Possible?
$1\ ^1S_0$	0^{-+}	yes
$1\ ^3S_1$ (ψ)	1^{--}	no
$1\ P_1$	1^{+-}	no
$1\ ^3P_0$	0^{++}	yes
$1\ ^3P_1$	1^{++}	yes
$1\ ^3P_2$	2^{++}	yes
$2\ ^1S_0$	0^{-+}	yes
$2\ ^3S_1$ (ψ')	1^{--}	no

Table II. X(3415) branching ratios.

Final state	$B(\gamma X) \times B(X \to \text{final state})$	$B(X \to \text{final state})$[a]
$\pi^+\pi^-\pi^+\pi^-$	$(3.2 \pm 0.6) \times 10^{-3}$	$(4.3 \pm 1.7)\%$
$\pi^+\pi^-K^+K^-$	$(2.7 \pm 0.7) \times 10^{-3}$	$(3.6 \pm 1.5)\%$
$\pi^+\pi^-\pi^+\pi^-\pi^+\pi^-$	$(1.4 \pm 0.5) \times 10^{-3}$	$(2 \pm 1)\%$
$\pi^+\pi^-$	$(0.7 \pm 0.2) \times 10^{-3}$	$(1 \pm 0.5)\%$
K^+K^-	$(0.7 \pm 0.2) \times 10^{-3}$	$(1 \pm 0.5)\%$
$\pi^+\pi^-p\bar{p}$	$(0.4 \pm 0.13) \times 10^{-3}$	$(0.5 \pm 0.2)\%$
$\psi\gamma$	$(2 \pm 2) \times 10^{-3}$	$(3 \pm 3)\%$

Resonance Production:

$$\frac{B(X \to \rho^0\pi^+\pi^-)}{B(X \to \pi^+\pi^-\pi^+\pi^-)} = 0.39 \pm 0.12$$

$$\frac{B(X \to K^*(891)K^\pm\pi^\mp)}{B(X \to \pi^+\pi^-K^+K^-)} = 0.41 \pm 0.10$$

a. Calculated using $B(\psi' \to \gamma X(3415)) = 0.075 \pm 0.026$.

Table III. X(3500) branching ratios.

Final state	$B(\gamma X) \times B(X \rightarrow \text{final state})$	$B(X \rightarrow \text{final state})$[a]
$\pi^+\pi^-\pi^+\pi^-$	$(1.1 \pm 0.4) \times 10^{-3}$	1.2%
$\pi^+\pi^- K^+K^-$	$(0.6 \pm 0.3) \times 10^{-3}$	0.7%
$\pi^+\pi^-\pi^+\pi^-\pi^+\pi^-$	$(1.7 \pm 0.6) \times 10^{-3}$	1.9%
$\pi^+\pi^-$ and K^+K^-	$< 0.15 \times 10^{-3}$	< 0.2%
$\pi^+\pi^- p\bar{p}$	$(0.1 \pm 0.08) \times 10^{-3}$	0.1%
$\psi\gamma$	$(24 \pm 8) \times 10^{-3}$	26%

Resonance Production:

$$\frac{B(X \rightarrow \rho^o\pi^+\pi^-)}{B(X \rightarrow \pi^+\pi^-\pi^+\pi^-)} = 0.24 \pm 0.20$$

$$\frac{B(X \rightarrow K^*(891)K^\pm\pi^\mp)}{B(X \rightarrow \pi^+\pi^- K^+K^-)} = 0.35 \pm 0.18$$

a. Calculated using $B(\psi' \rightarrow \gamma X(3500)) = 0.09$ from Ref. 5. The sum of all uncertainties being rather large, these figures are to be considered estimates and no errors are quoted.

Table IV. X(3550) branching ratios.

Final state	$B(\gamma X) \times B(X \rightarrow \text{final state})$	$B(X \rightarrow \text{final state})$[a]
$\pi^+\pi^-\pi^+\pi^-$	$(1.6 \pm 0.4) \times 10^{-3}$	2%
$\pi^+\pi^- K^+K^-$	$(1.4 \pm 0.4) \times 10^{-3}$	1.8%
$\pi^+\pi^-\pi^+\pi^-\pi^+\pi^-$	$(0.8 \pm 0.5) \times 10^{-3}$	1%
$\pi^+\pi^-$ and K^+K^-	$(0.2 \pm 0.1) \times 10^{-3}$	0.2%
$\pi^+\pi^- p\bar{p}$	$(0.2 \pm 0.1) \times 10^{-3}$	0.2%
$\psi\gamma$	$(10 \pm 6) \times 10^{-3}$	12%

Resonance Production:

$$\frac{B(X \rightarrow \rho^o\pi^+\pi^-)}{B(X \rightarrow \pi^+\pi^-\pi^+\pi^-)} = 0.31 \pm 0.17$$

$$\frac{B(X \rightarrow K^*(891)K^\pm\pi^\mp)}{B(X \rightarrow \pi^+\pi^- K^+K^-)} = 0.25 \pm 0.13$$

a. Calculated using $B(\psi' \rightarrow \gamma X(3550) = 0.08$ from Ref. 5. The comment about errors given in Table III also applies here.

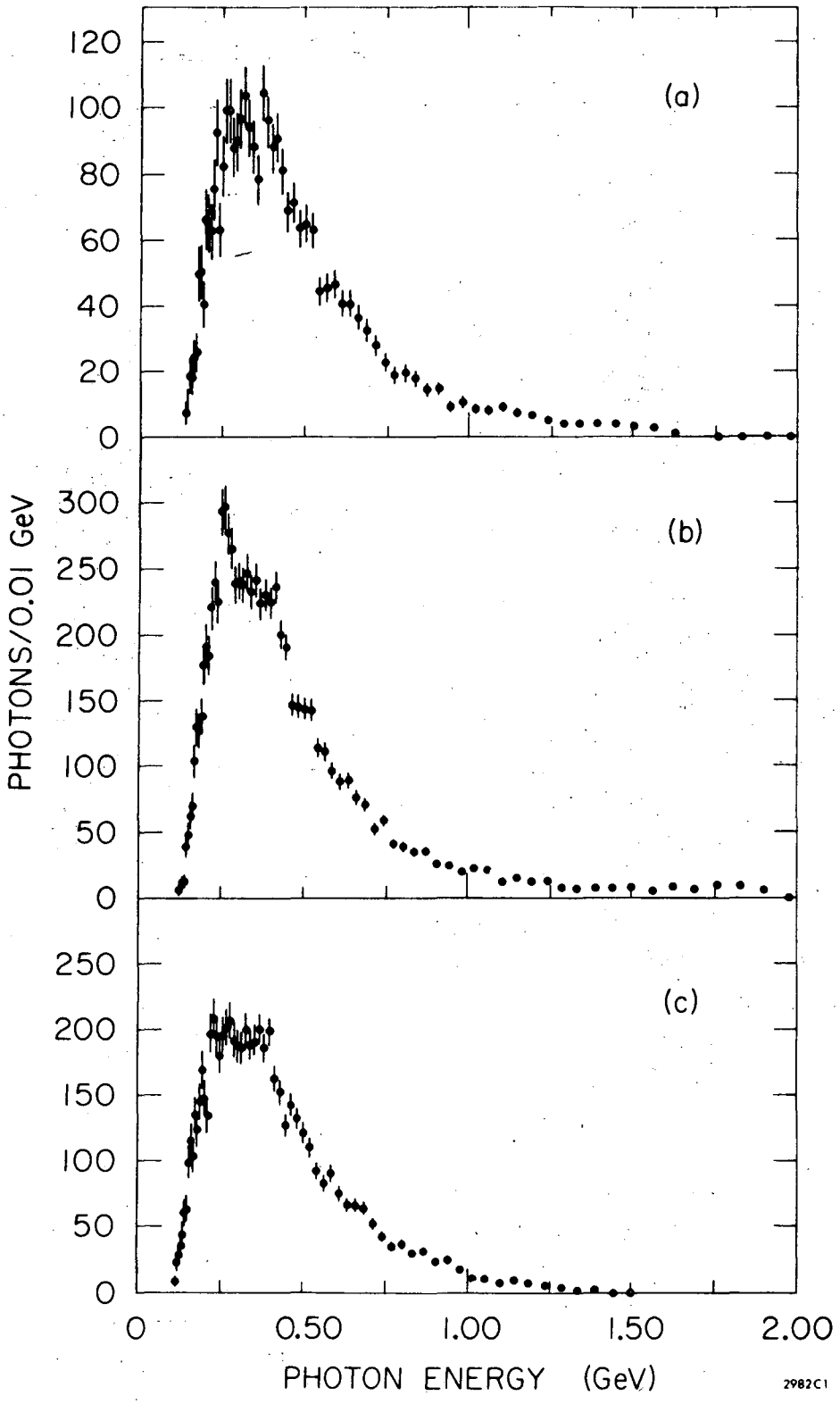

Fig. 1. Inclusive photon energy spectrum from (a) ψ decays, (b) ψ' decays, (c) Monte-Carlo calculation for ψ decays.

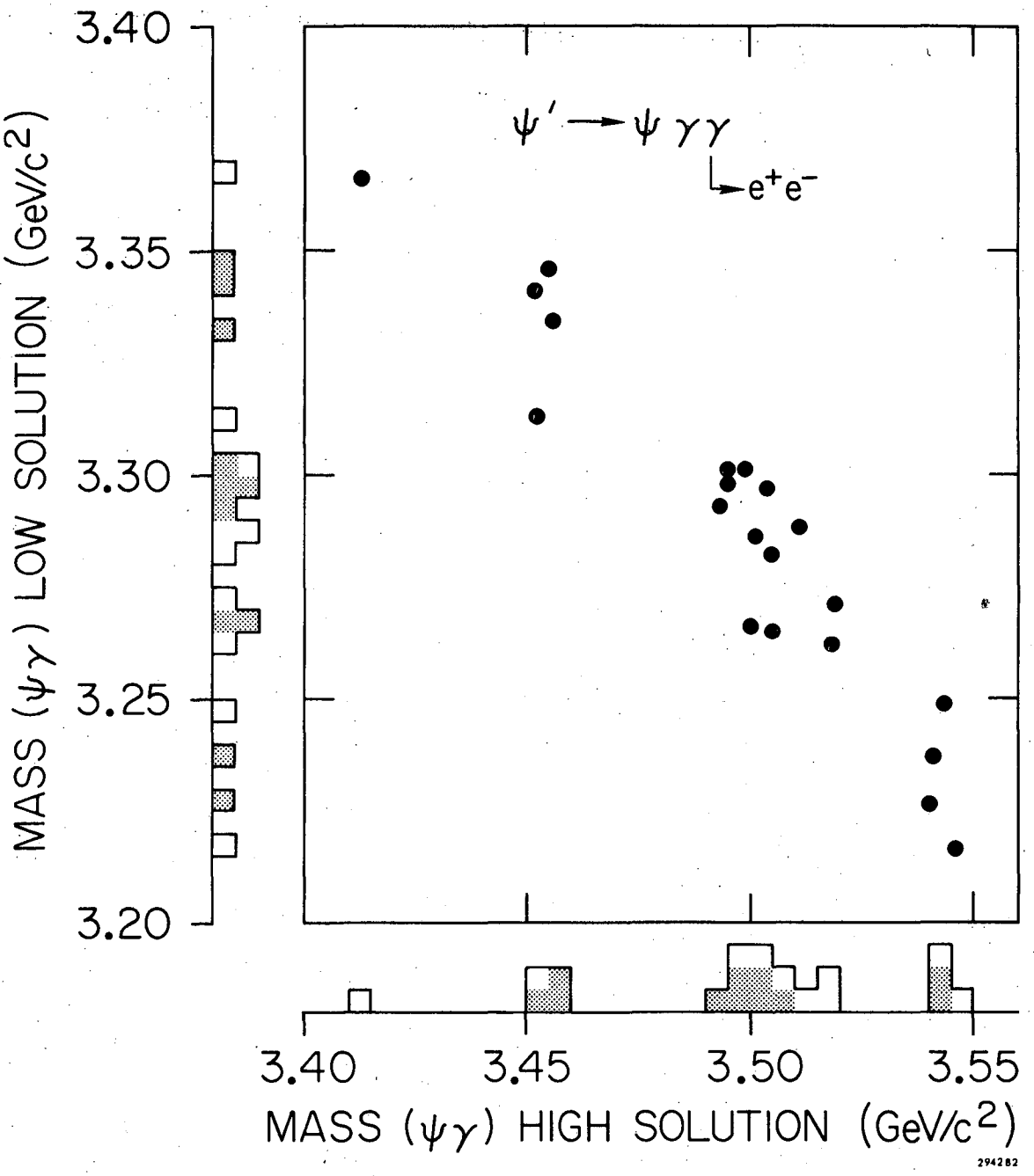

Fig. 2. Scatter plot of the two $\psi\gamma$ mass combinations from the process $\psi' \rightarrow \gamma\gamma\psi$.

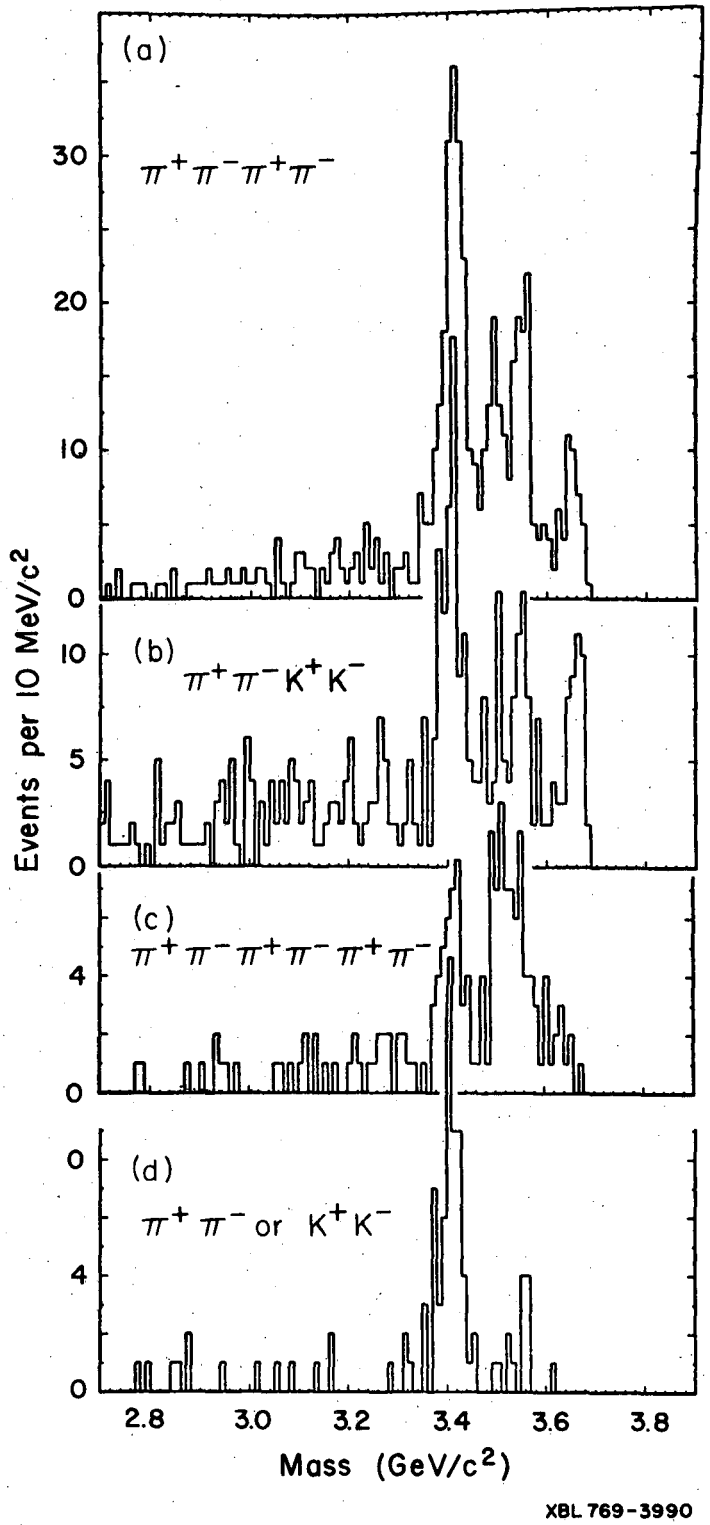

Fig. 3. Mass spectrum for multihadron states X fit to the reaction $\psi' \rightarrow \gamma X$ with X being (a) $\pi^+\pi^-\pi^+\pi^-$, (b) $\pi^+\pi^-K^+K^-$, (c) $\pi^+\pi^-\pi^+\pi^-\pi^+\pi^-$, (d) $\pi^+\pi^-$ or K^+K^-.

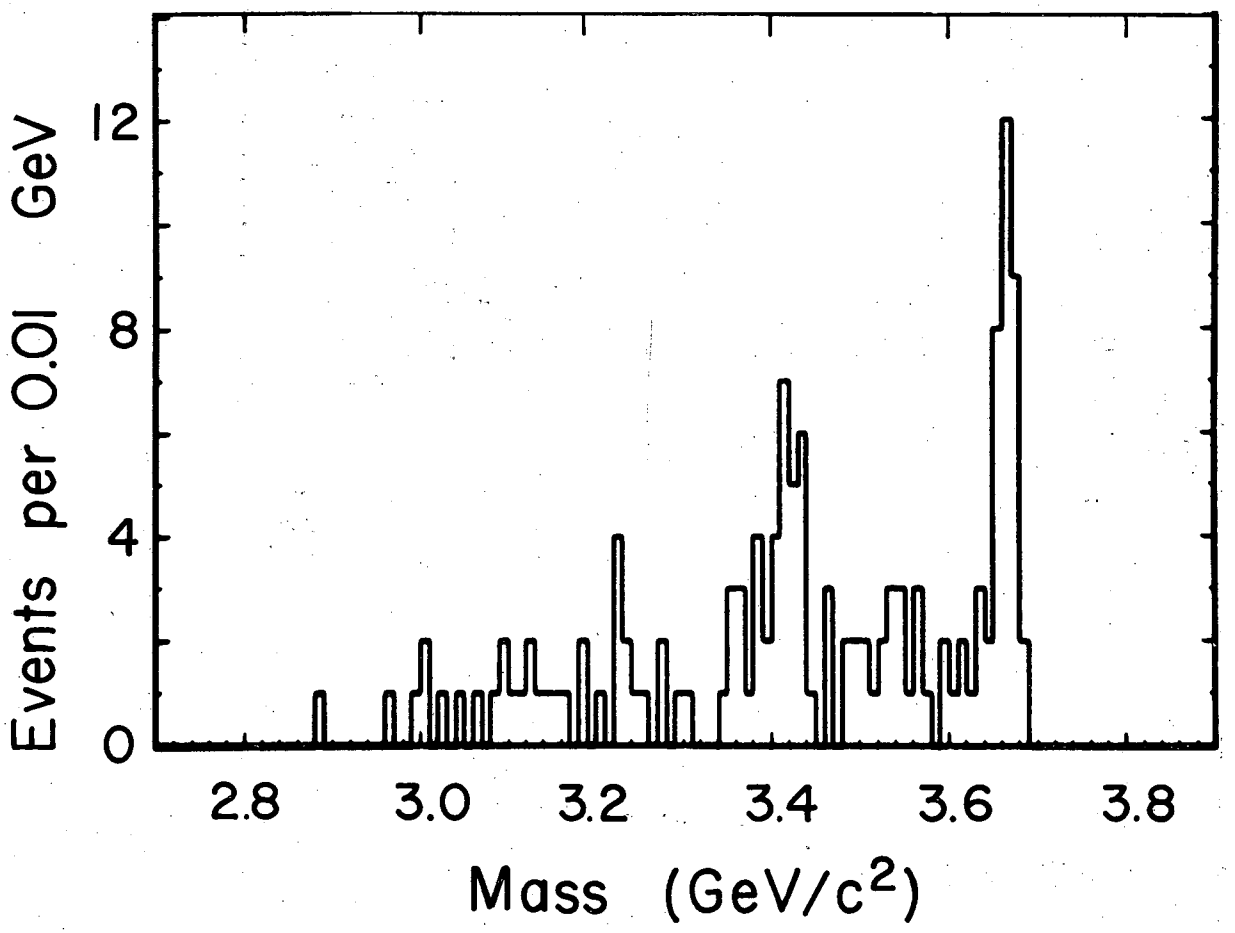

XBL769-3997

Fig. 4. Mass spectrum of $\pi^+\pi^-p\bar{p}$ for events fit to the reaction $\psi' \rightarrow \gamma\pi^+\pi^-p\bar{p}$.

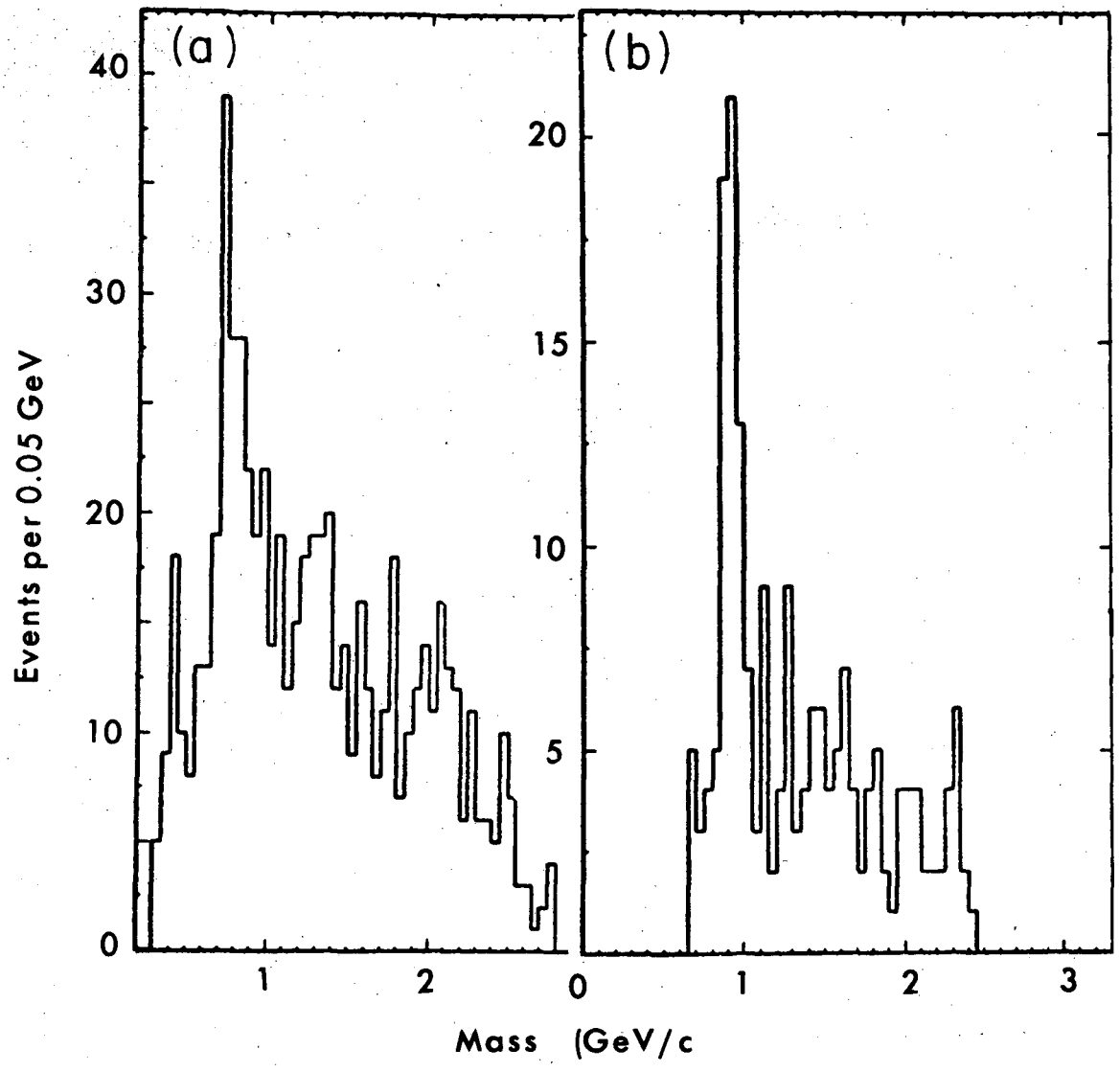

Fig. 5. (a) $\pi^+\pi^-$ mass spectrum from $X(3415) \rightarrow \pi^+\pi^-\pi^+\pi^-$ (four combinations per event); (b) $K^\pm\pi^\mp$ mass spectrum from $X(3415) \rightarrow \pi^+\pi^-K^+K^-$ (two combinations per event).

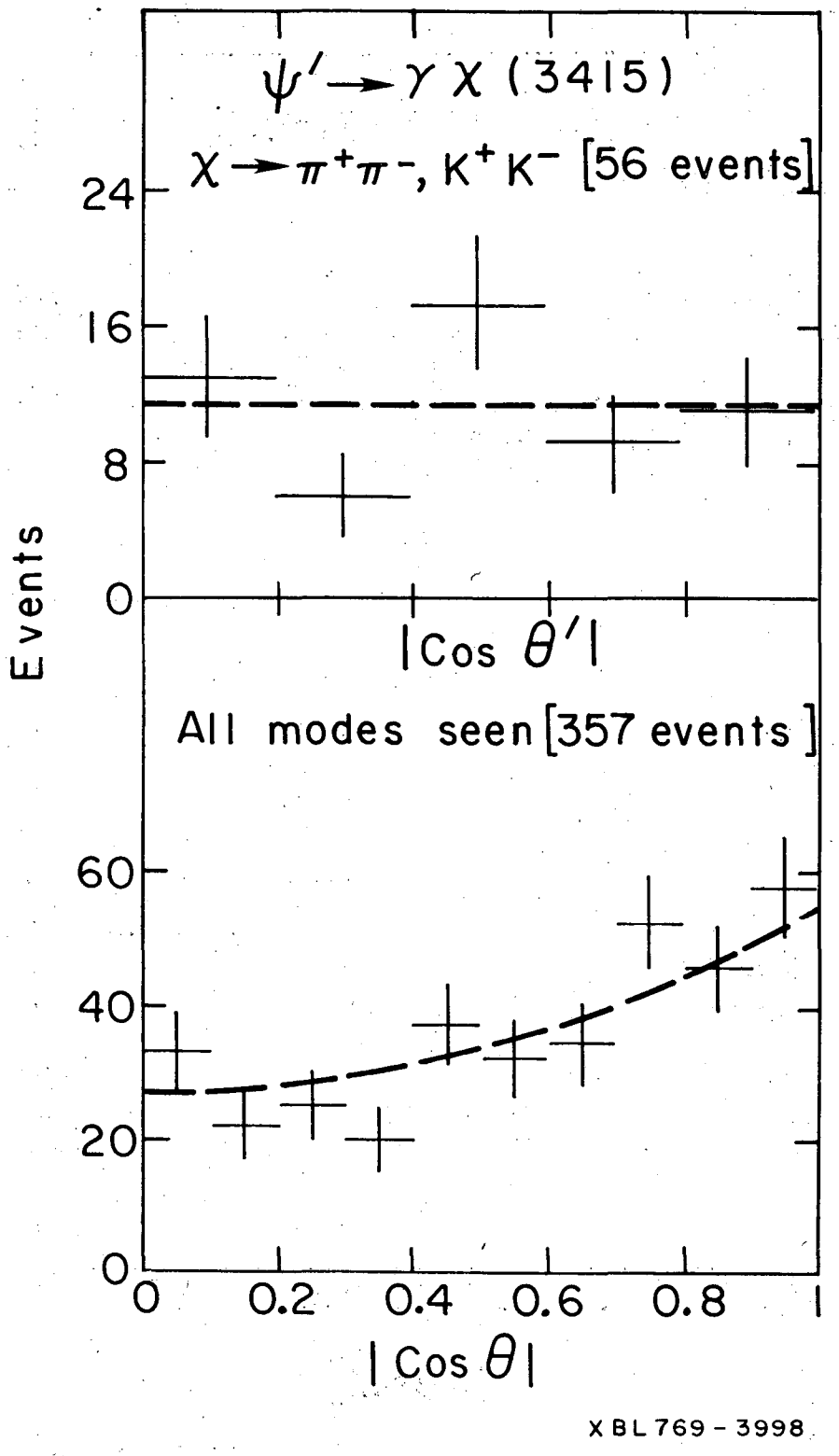

Fig. 6. Decay angular distributions for X(3415). Angles are defined in text and dashed lines represent prediction for J = 0.

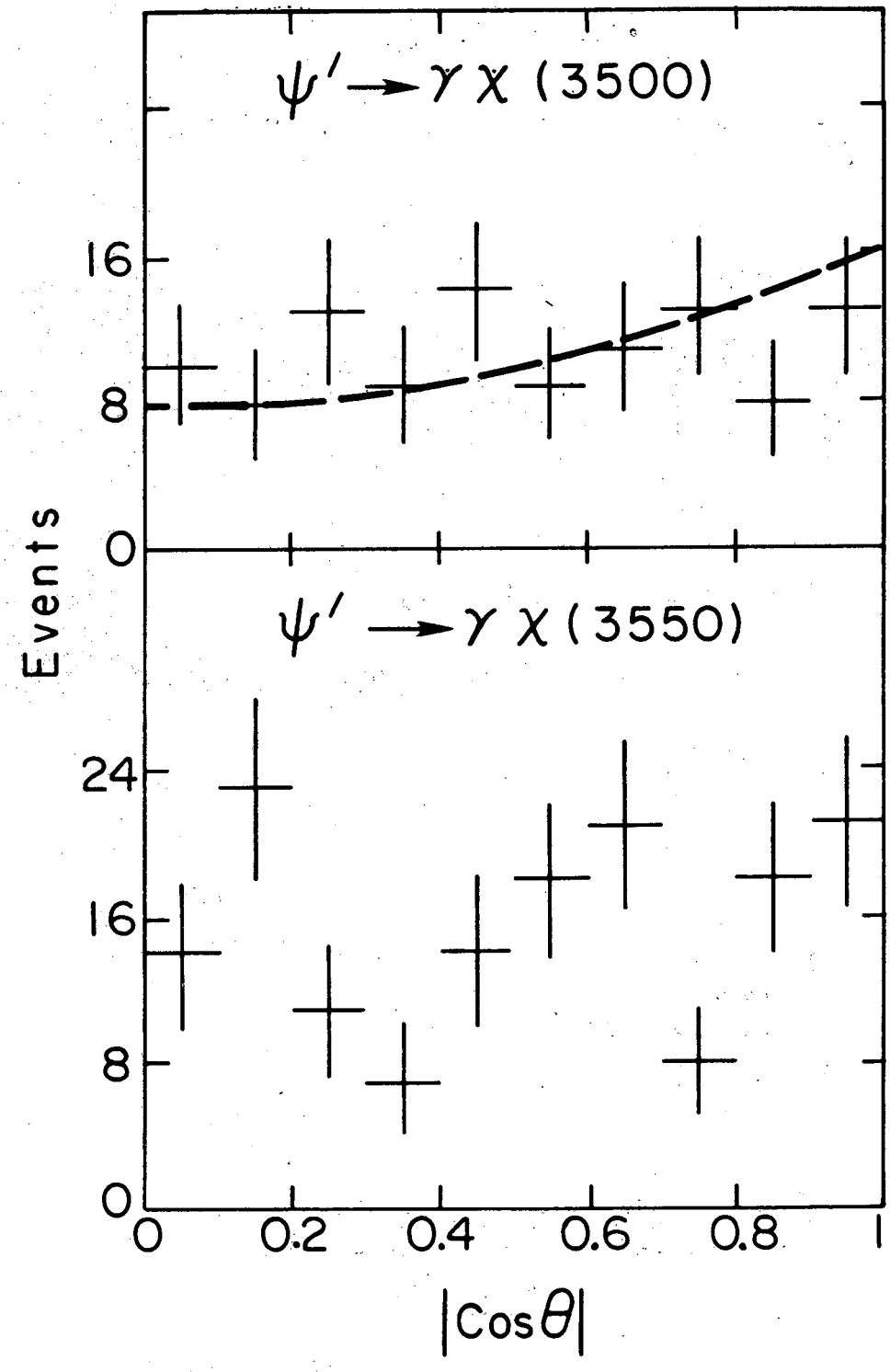

XBL769-3995

Fig. 7. Angular distributions for (a) X(3500) and (b) X(3550). Dashed line represents prediction for J = 0.

TECHNICAL INFORMATION DIVISION
LAWRENCE BERKELEY LABORATORY
UNIVERSITY OF CALIFORNIA
BERKELEY, CALIFORNIA 94720